Molecular Biotechnology
https://doi.org/10.1007/s12033-018-0078-3

ORIGINAL PAPER

Optimization of a Bioluminescence Resonance Energy Transfer-Based Assay for Screening of *Trypanosoma cruzi* Protein/Protein Interaction Inhibitors

Jesica G. Mild[1,2] · Lucia R. Fernandez[1,2] · Odile Gayet[3] · Juan Iovanna[3] · Nelson Dusetti[3] · Martin M. Edreira[1,2,4]

Abstract

Chagas disease, a parasitic disease caused by *Trypanosoma cruzi,* is a major public health burden in poor rural populations of Central and South America and a serious emerging threat outside the endemic region, since the number of infections in non-endemic countries continues to rise. In order to develop more efficient anti-trypanosomal treatments to replace the outdated therapies, new molecular targets need to be explored and new drugs discovered. *Trypanosoma cruzi* has distinctive structural and functional characteristics with respect to the human host. These exclusive features could emerge as interesting drug targets. In this work, essential and differential protein–protein interactions for the parasite, including the ribosomal P proteins and proteins involved in mRNA processing, were evaluated in a bioluminescence resonance energy transfer-based assay as a starting point for drug screening. Suitable conditions to consider using this simple and robust methodology to screening compounds and natural extracts able to inhibit protein–protein interactions were set in living cells and lysates.

Keywords *Trypanosoma cruzi* · BRET · Protein–protein interactions · Drug screening

Introduction

Protein–protein interactions (PPIs) are known to play important roles in a wide range of biological processes, for example, signaling transduction, gene expression, cell proliferation and differentiation, morphology, motility, and apoptosis. Several approaches to study PPIs have been described. Classical strategies include biochemical and genetic methods, such as: chemical cross-linking, combined fractionation during chromatography, co-immunoprecipitation, and later, high-throughput methods like yeast two-hybrid, phage display, and tandem affinity purification–MS [1]. However, most of the conventional methods used to study PPIs are unable to provide information of the spatial–temporal distribution of interactions. To overcome these limitations, newer reporter gene-based strategies, like bimolecular fluorescence complementation (BiFC), fluorescence resonance energy transfer (FRET), and bioluminescence resonance energy transfer (BRET), have been developed [2]. Fluorescent-based techniques provide noninvasive methods to study PPIs in the native environment of the living cell, allowing real-time qualitative and quantitative measurements of dynamic events.

Jesica G. Mild and Lucia R. Fernandez have contributed equally to this work.

Electronic supplementary material The online version of this article (https://doi.org/10.1007/s12033-018-0078-3) contains supplementary material, which is available to authorized users.

✉ Martin M. Edreira
mme2@pitt.edu

1 Universidad de Buenos Aires, Facultad de Ciencias Exactas y Naturales, Departamento de Química Biológica, Buenos Aires, Argentina

2 CONICET - Universidad de Buenos Aires, Instituto de Química Biológica de la Facultad de Ciencias Exactas y Naturales (IQUIBICEN), Buenos Aires, Argentina

3 Centre de Recherche en Cancérologie de Marseille (CRCM), INSERM U1068, CNRS UMR 7258, Institut Paoli-Calmettes, Aix Marseille Université, Marseille, France

4 Intendente Guiraldes 2140, Ciudad Universitaria, Pabellón 2, 2do Piso, CM1, 1428 Ciudad de Buenos Aires, Argentina

Published online: 29 March 2018

In addition to quantitative measurement of PPIs, BRET-based assays have been used to screen new receptor ligands and inhibitors of disease-related proteases [3]. Furthermore, since PPIs could play a crucial function in a human pathological process, disrupting essential interactions could affect cell viability and lead to cell death. For this reason, target-driven screening of compounds with the ability of disrupting PPIs has emerged as a viable approach in drug discovery, and high-throughput screening assay based on BRET is a well-suited method to search for such inhibitory compounds [4, 5].

Current treatment of Chagas disease is based on only two drugs, nifurtimox and benznidazole, introduced in the early 1970s. Drugs are efficient in the acute phase of the infection, but could present severe side effects and limited efficacy during the chronic stage of the disease [6]. In this regard, a consensus has emerged that persistent parasitism plays central role in the pathogenesis of the chronic cardiomyopathy [6]. Therefore, there is an urgent need for new drugs and targets, to develop new anti-trypanosomal treatments with higher efficiency, especially during the chronic phase of the infection.

Trypanosoma cruzi, the protozoan parasite etiologic agent of Chagas disease, has distinctive biological processes, with macromolecular structures and functional characteristics that differ from the ones present in the human host. Consequently, PPIs that are essential for cell viability and are exclusive to the parasite, or significantly different from its human counterpart, emerge as interesting anti-parasitic drug targets. In this work, we used previously described interactions between proteins from *T. cruzi* that shown to have differential features, in a BRET-based interaction assay as a starting point for drug screening.

BRET assays have been performed using cell lysates, live cells, or animal model [2, 7–10]. Typically, energy is transferred from the donor (luciferase) to an acceptor (usually a fluorescent protein) [11]. To meet the conditions of energy transfer, the emission spectrum of the donor must overlap the excitation spectrum of the acceptor, for resonance energy transfer to occur. In addition, donor and acceptor should be in close proximity, since it has been shown that energy transfer progressively decreases when the distance between them increases from 1 to 10 nm, with 10 nm the maximum distance for energy transfer to occur [12, 13]. Even when the wavelengths overlap and the distance is optimal, the relative spatial orientation of the donor and the acceptor with respect to each other is absolutely crucial for energy transfer to occur [14].

The study of PPIs through this method involves separately fusion of the interacting partners to an energy donor and an energy acceptor. When the interaction takes place, donor and acceptor are brought into close proximity, and if the proper spatial orientation is reached, resonance energy transfer occurs [15]. For this end, a Renilla luciferase protein (Rluc) was used as energy donor and an enhanced variant of the yellow fluorescent protein (EYFP) as the energy acceptor. By oxidizing a substrate such as coelenterazine, Rluc produces light with a peak at 480 nm [16] and EYFP, the resonance energy transducer of the energy from Rluc, subsequently emits at 530 nm [11]. In this work, *T. cruzi* protein–protein interactions, including the ribosomal P proteins and proteins involved in mRNA processing, were evaluated in a BRET-based assay as a starting point for drug screening (Table 1).

The ribosomal P proteins form a lateral protuberance in the large subunit of the eukaryotic ribosome, called the stalk. This structure is involved in the translation step through interaction with the elongation factor 2 (EF-2) [17]. In *T. cruzi*, the stalk is composed of five different P proteins: TcP0, of about 34 kDa, containing a C-terminal end that deviates from the eukaryotic P consensus and bears similarity with Archaea L10 protein, and four 11 kDa proteins, TcP1α, TcP1β, TcP2α, TcP2β, with the typical eukaryotic P consensus sequence at their C-terminal end which present differential interactions [18–20]. A differential pattern of protein–protein interactions has been proposed for the parasite [19, 20].

Protein-coding genes in *T. cruzi* are transcribed into polycistronic RNAs. To generate individual transcripts, pre-mRNAs are then processed by 5′ trans-splicing and 3′ polyadenylation [21]. The trans-splicing process is also an interesting mechanism to exploit as a potential drug target, since it differs from the process in most eukaryotes [22]. In eukaryotes, the earliest assembly phase of the spliceosome involves the formation of the E complex. Within the E complex are the splicing factors SF1 and U2AF that associate cooperatively with pre-mRNA and play a crucial role in 3′ splice site recognition [23]. In *trypanosomatids*, the SF1 recognizes the branch point sequence, while the splicing factor U2AF, a heterodimer composed of a 65 kDa (U2AF65) and a 35 kDa (U2AF35) subunits, contacts the polypyrimidine tract and the AG splice site, respectively, [24]. As for other eukaryotes, a strong interaction between U2AF65 and SF1 has been shown for *T. cruzi*, even when these proteins have significant differences compared to the mammalian orthologous [25]. Following E complex formation, SF1 is displaced from the complex and replaced by association of SF3b14a/p14 that recognizes the adenosine at the branch point [23]. Using yeast two hybrid assays, it has been demonstrated that TcSF3b155 and Tcp14 interacted strongly with each other and, in particular, *T. cruzi* SF3b155 interface appeared to be larger, with more complex elements than in humans [26]. In line with these observations, it has been suggested the possibility of exploiting species-specific features in SF3b to find compounds with anti-parasitic activity [27]. Another strong essential interaction interesting to study further has been found between TcFIP1-like and TcCPSF30, components of the polyadenylation complex. In trypanosomatids

Table 1 *T. cruzi* PPIs included in this work as targets for the development of a BRET-based assay for screening of interaction inhibitors

Interacting proteins	Gene ID (TritrypDB)	Identity to human (%)	Protein localization
P0	TcCLB.508,355.260	41	Ribosomal stalk
P1α	TcCLB.510,823.70	46	
P0	TcCLB.508,355.260	41	Ribosomal stalk
P1β	TcCLB.510,267.20	39	
P0	TcCLB.508,355.260	41	Ribosomal stalk
P2α	TcCLB.505,977.26	34	
P0	TcCLB.508,355.260	41	Ribosomal stalk
P2β	TcCLB.509,165.40	32	
P1α	TcCLB.510,823.70	46	Ribosomal stalk
P2β	TcCLB.509,165.40	32	
P2α	TcCLB.505,977.26	34	Ribosomal stalk
P2β	TcCLB.509,165.40	32	
SF1	TcCLB.508,717.40	27	Trans-splicing E complex
U2AF65	TcCLB.510,265.40	22	
FIP1	TcCLB.510,351.80	44	Polyadenylation complex
CpsF30	TcCLB.510,219.30	47	
p14	TcCLB.510,105.33	42	Trans-splicing A complex
Sf3b155	TcCLB.508,827.100	33	
Mago	TcCLB.506,945.200	53	Exon junction complex
Y14	TcCLB.507,515.40	29	

and humans, CPSF30 and FIP1 proteins share a common surface of interaction with conserved residues, but the contact interface has substantial modifications between them [28]. The exon junction complex is involved in mRNA splicing, transport, and translation. Four proteins constitute the core of the EJC: eIF4A3, MAGO, Y14, and MLN51. MAGOH and Y14 form a tight heterodimer that coevolved in eukaryotes, demonstrating the functional requirement for their heterodimerization [29]. However, it has been proposed that trypanosomes might contain a modified form of exon junction complex, containing Mago, a divergent Y14, and a novel protein with an NTF2 domain. The lack of any association with nuclear eIF4AIII, interestingly, correlates with the fact that two out of three residues required for Y14 to interact with eIF4AIII are mutated [30].

In this work, we established suitable conditions to consider using bioluminescence resonance energy transfer (BRET) for screening of natural extracts and compounds able to inhibit essential and exclusive *T. cruzi's* PPIs in living cells and lysates.

Results

Generation of Fusion Proteins

In order to detect a positive BRET signal, an efficient energy transfer should take place between partners of an interaction. For this to happen, donor and acceptor need to be within a 10-nm-range distance with a correct orientation of the donor/acceptor dipoles. Consequently, the absence of BRET signal does not imply the lack of interaction, more likely, that the interaction failed to achieve the necessary proximity between the donor and acceptor and/or the relative orientation of the dipoles. For each partner of the PPI, there are four different fusion configurations, with Rluc or EYFP in N-terminus or C-terminus localization. Since there is no reliable way to predict which configuration would produce the maximum transfer of resonance energy, all possible configurations and combinations should be tested [15]. For this reason, every protein was subcloned into the four different BRET destination vectors, obtaining fusions of each protein of interest to the donor (Rluc) and acceptor (EYFP) in N- and C-terminal (Fig. 1). Briefly, ORFs corresponding to all interactions partners (Table 1) were amplified from genomic DNA of epimastigotes of the CL Brener strain and cloned into a Gateway® entry vector system (pCR ®8/GW/TOPO®TA). For P1α, P1β, P2α, P2β, SF1, FIP1, CpsF30, p14, Y14, and Mago, the full length coding sequence was cloned. In the case of P0, Sf3b155, U2AF65, sequences corresponding to the interaction domains were cloned, in order to facilitate expression (P0: 212-323 residues; U2AF65: 614-841 residues; Sf3b155: residues 1-270) [25, 26, 31]. Each ORF was later subcloned by LR recombination reaction to four different BRET destination vectors.

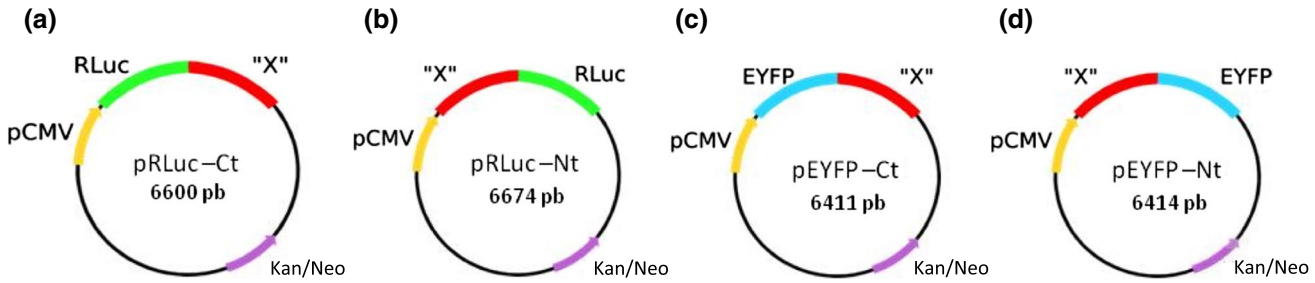

Fig. 1 Schematic representation of BRET destination vectors. Genes of interest (X) were subcloned into the four possible configurations, in order to obtain C- and N-terminal fusions to Rluc **(a, b)** and EYFP **(c, d)**

BRET in Live Cells

Donor Saturation Curves

To verify the configuration and combination of fusion proteins that produce the highest BRET signal, for each PPI, eight possible combinations were evaluated in donor saturation assays in HEK 293T cells. For aim, cells were transfected with a constant concentration of plasmid carrying the donor fusion and increasing concentrations of the vector coding for the acceptor fusion. Data obtained in saturation assays for ribosomal proteins and proteins that participate in the processing of mRNA, Figs. 2 and 3, respectively, showed that only some of the tested combinations presented a positive specific BRET signal, considering those specific curves where BRET values increased in a hyperbolic fashion. Although known interactions were analyzed, it was evident from the results that not every combination could reach the required spatial conformation for energy transfer (Supplementary Figures 1 and 2). Noteworthily, successful BRET signal for P proteins was obtained with one of the partners always in the Rluc conformation and the other partner in the EYFP conformation, independently of the N- or C-terminal localization of the fusion. When switching conformations, there was a decrease in the signal (Fig. 2) or not specific signal at all (Supplementary Figure 1). In the case of proteins that participate in the processing of mRNA, swapping conformations had a similar result (Fig. 3 and Supplementary Figure 2).

BRET from Lysates

Donor Saturation Curves

As an alternative to BRET in living cells, BRET was performed using lysates obtained from cells transfected with donor and acceptor fusions. For this aim, HEK293T cells were separately transfected with donor or acceptor fusion proteins and mechanically lysed 48 h post-transfection. A constant concentration of donor, corresponding to 150,000 RLU (Relative Luciferase Units), and increasing concentrations of the acceptor proteins were used in donor saturation assay. Overall, BRET signal from lysates was lower than signal obtained from complete cells. Furthermore, while positive hyperbolic BRET signal was obtained for P0/P1α, P0/P1β, P0/P2α, and P1α/P2β (Figs. 4a–d, respectively), no hyperbolic BRET signal was observed for the tested combinations of P0/P2β (Supplementary Figure 3). Noteworthily, for some combinations that presented no BRET signal in living cells, a positive hyperbolic signal was observed from lysates. Inversely, BRET positive signal from living cells observed for some combinations was lost in lysates. Similar results were observed for mRNA processing proteins (Fig. 5 and Supplementary Figure 4). These observations strongly suggested that lysis conditions played an important role in the folding of proteins. The disturbance of the folding had a clear impact on the protein complex formation and the BRET signal. For this reason, it was not possible to establish a correspondence between BRET assays performed in living cells and cellular lysates.

A suitable system for the screening of small molecules with the ability of disrupting PPIs would be a system that could be turned off in the presence of these inhibitors. As a proof of principle, the BRET assay for the interaction Sf3b155$^{1\text{-}270}$-Rluc/p14-EYFP was performed in the presence of a bacterially expressed and purified His-Sf3b155$^{1\text{-}270}$ as a competitor. As shown in Fig. 6, a significant reduction in the BRET signal for Sf3b155$^{1\text{-}270}$-Rluc/p14-EYFP confirms that it is possible to detect by means of the BRET assay an inhibition of the target interaction.

Discussion

Compounds capable of inhibiting essential protein interactions and affecting parasite's viability could be used as the basis for the development of new drugs against Chagas disease. Following this principle, targeting the interface of the *T. cruzi's* triosephosphate isomerase, a homodimeric enzyme catalytically active only as a dimer, has been proposed for

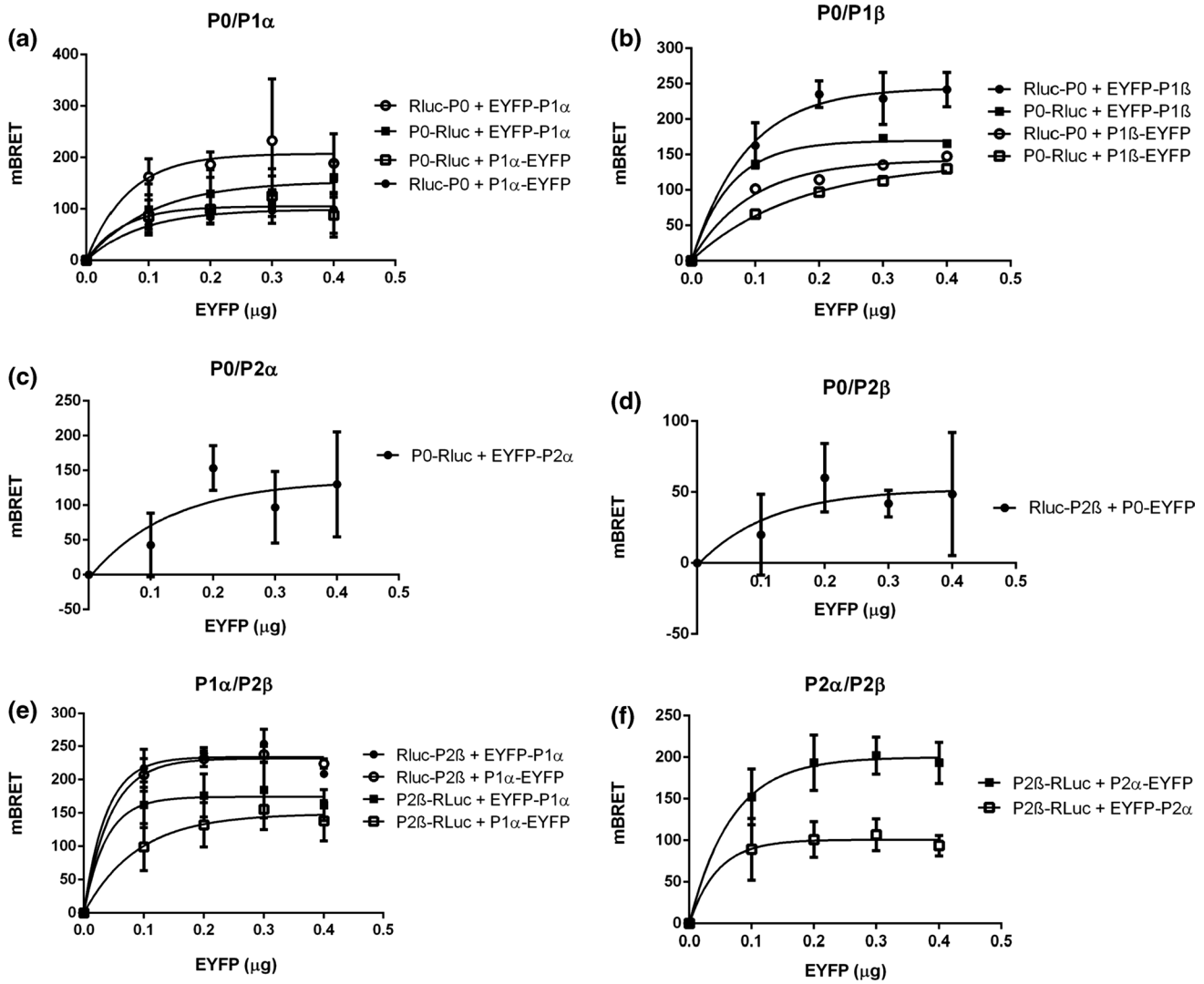

Fig. 2 Donor saturation curves in living cells for P proteins interactions. Cells were co-transfected with a fixed amount of donor vector (0.4 μg) and increasing concentrations of acceptor vector (0.1; 0.2; 0.3; and 0.4 μg). Light emitted at donor and acceptor wavelengths was measured 48 h post-transfection. Background signal was calculated from cells transfected with donor-fused partner vector and empty acceptor vector. **a** $P0^{212\text{-}323}$/P1α, **b** $P0^{212\text{-}323}$/P1β, **c** $P0^{212\text{-}323}$/P2α, **d** $P0^{212\text{-}323}$/P2β, **e** P1α/P2β, **f** P2α/P2β. Data show mean ± SD from three independent experiments

the design of molecules that disturb the contacts between subunits [32]. In fact, it has been demonstrated that low molecular weight compounds, which bind to the dimer interface perturbing the association between the two monomers, abolish its function with a high level of selectivity and lead to parasite death [33–35]. Additionally, not only the inhibition of the dimer formation could have anti-parasitic properties. A series of symmetrical molecules, which may stabilize the dimer and prevent the movement necessary for catalysis, were recently described as highly potent and selective *T. cruzi* growth inhibitors [36].

The screening of small compounds affecting the PPI should be accomplished by a sensitive, reliable, easy to perform, and inexpensive method. Given these requirements, BRET would be a suitable screening method. In this work, PPIs having unique functional or structural roles in essential processes in the parasite were selected to set up a BRET-based screening in living cells and cell lysates. Since there was no reliable way to predict the configuration and combination of the interacting proteins that were going to show the highest BRET signal, each protein of the PPI had to be fused with the donor and the acceptor (Rluc and EYFP, respectively), in N- and C-terminals. Therefore, eight possible configurations for each PPI were tested in donor saturation assays. Taking into account that in a BRET-based screening assay, the BRET signal has to be high enough to provide sufficient signal output for the detection of the interaction and a decrease in the signal, due to the interruption of that

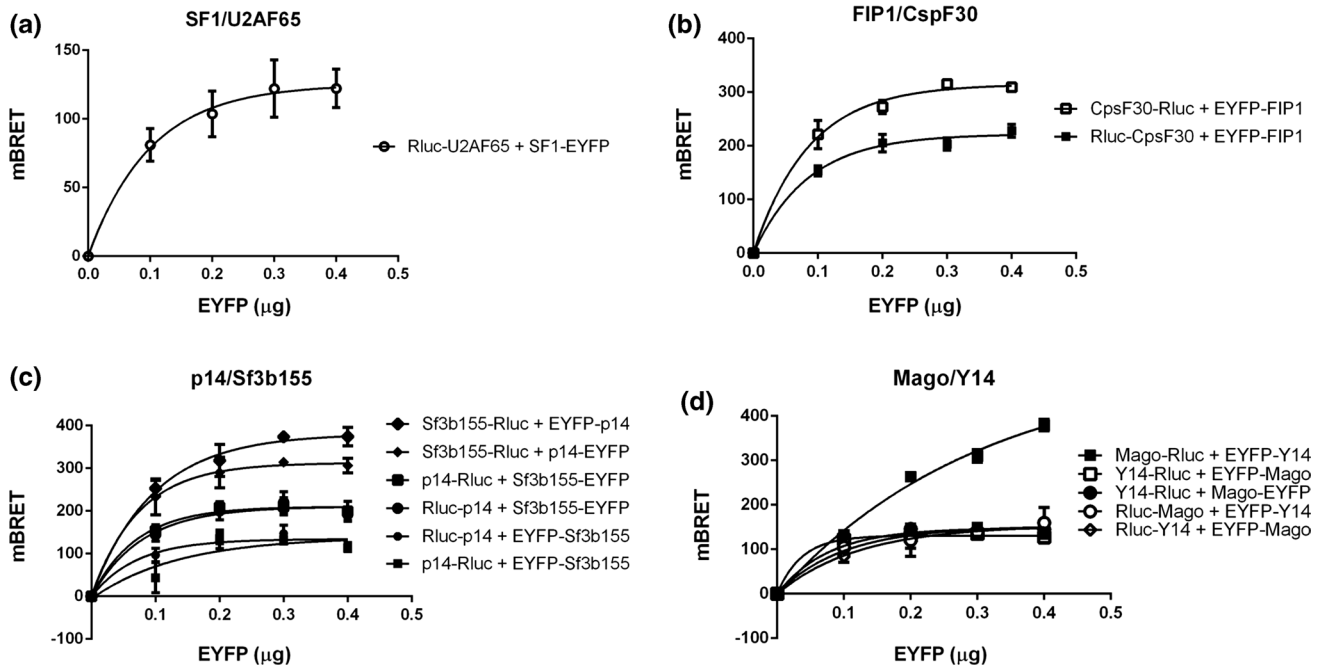

Fig. 3 Donor saturation curves in living cells for interaction between proteins that take part in the processing of mRNA. Cells were co-transfected with a fixed amount of donor vector (0.4 μg) and increasing concentrations of acceptor vector (0.1; 0.2; 0.3; and 0.4 μg). Light emitted at donor and acceptor wavelengths was measured 48 h post-transfection. Background signal was calculated from cells transfected with donor-fused partner vector and empty acceptor vector. **a** SF1/U2AF65$^{614\text{-}841}$, **b** FIP1/CpsF30, **c** p14/Sf3b155$^{1\text{-}270}$, **d** Mago/Y14. Data show mean ± SD from three independent experiments

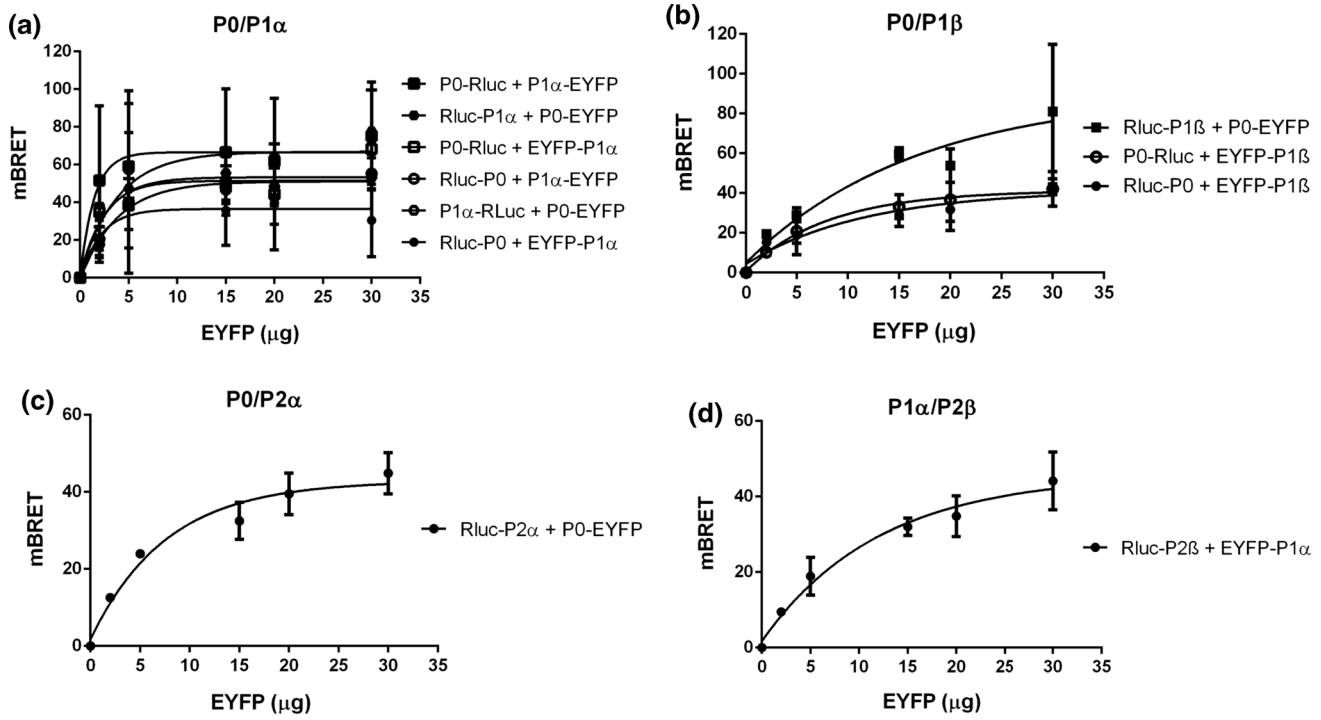

Fig. 4 Donor saturation curves using lysates containing P proteins. Protein concentration corresponding to 150.000 RLU of luciferase activity was incubated with increasing concentrations of acceptor (5, 15, 20, and 30 μg): **a** P0$^{212\text{-}323}$/P1α, **b** P0$^{212\text{-}323}$/P1β, **c** P0$^{212\text{-}323}$/P2α, **d** P0$^{212\text{-}323}$/P2β, **e** P1α/P2β. Data show mean ± SD from three independent experiments

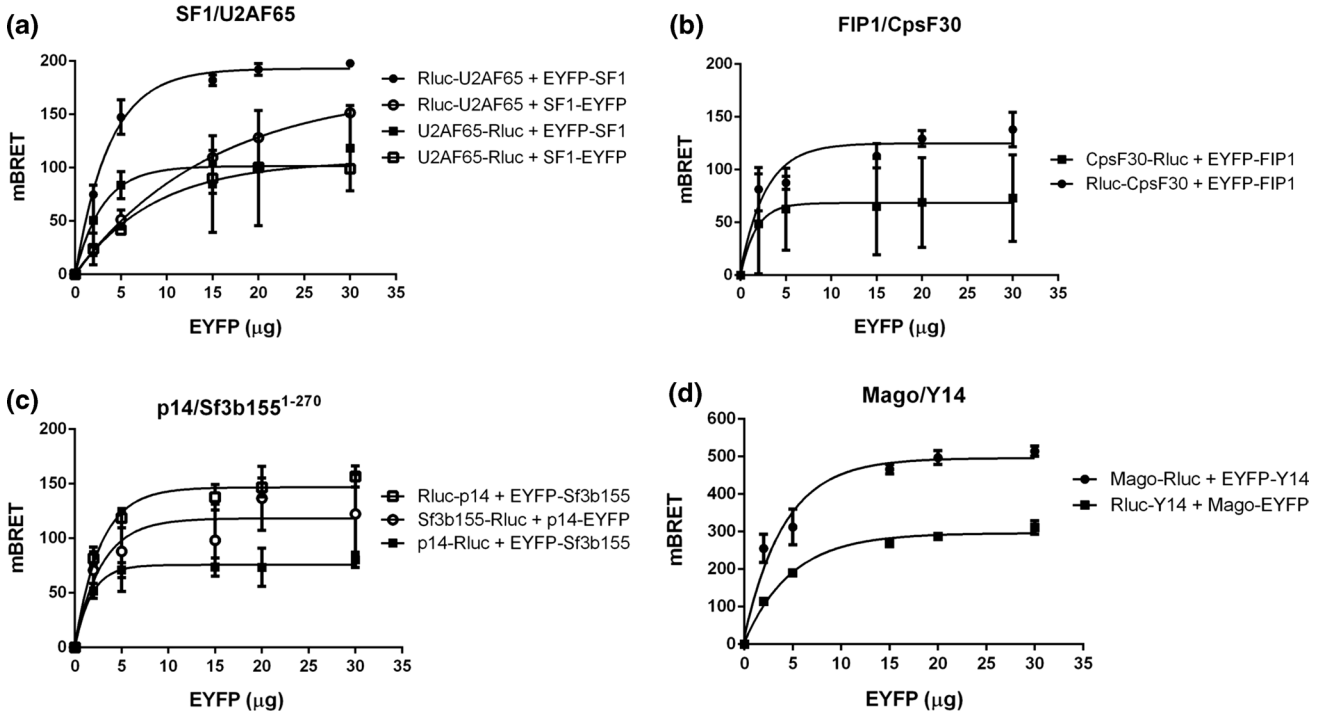

Fig. 5 Donor saturation curves using lysates containing proteins that take part in the processing of mRNA. Protein concentration corresponding to 150.000 RLU of luciferase activity was incubated with increasing concentrations of acceptor (5, 15, 20, and 30 μg): **a** SF1/U2AF65$^{614\text{-}841}$, **b** FIP1/CpsF30, **c** p14/Sf3b155$^{1\text{-}270}$, **d** Mago/Y14. Data show mean ± SD from three independent experiments

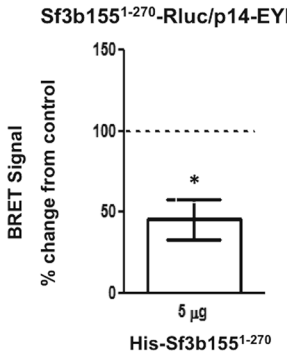

Fig. 6 Displacement of the Sf3b155$^{1\text{-}270}$-Rluc/p14-EYFP interaction. Sf3b155$^{1\text{-}270}$-Rluc and 20 μg of p14-EYFP lysate were incubated in the presence of 5 μg of purified His-Sf3b155$^{1\text{-}270}$. Results are expressed as the percentage of the BRET signal for the interaction in the absence of His-Sf3b155$^{1\text{-}270}$. Data represent the mean ± SD of three independent experiments. *$p < 0.05$, with unpaired Student's *t* test

interaction, we empirically considered 50 mBRET as a positive BRET signal.

In a first approach, the saturation assays were performed in living cells. All tested PPIs presented positive BRET signal for at least one combination of donor/acceptor, confirming that this technology was able to detect all previously reported interactions [25, 26, 28, 30, 31]. Considering these facts, it is possible to assume that combinations presenting no BRET signal constitute false negatives, probably, as a consequence of the spatial conformation adopted by the fusion proteins.

In this context, natural products or compounds derived from them are an important source of new therapeutic drugs. Consequently, one of our goals was to develop a BRET-based screening methodology that could be used for the screening of PPIs inhibitors from raw extracts of natural origin. As raw extracts are extremely complex since they are made of a highly heterogeneous mixture of compounds, we considered that the screening in lysates would be more appropriate than in living cells. For screening in living cells, compounds in the extract should be permeable to the plasma membrane, resistant to cell degradation, and more importantly, the extract non-toxic for cells. However, these conditions could not be predicted for the crude extracts. Working with lysates expressing the PPI partners would allow us to evaluate the ability of the extract to interrupt the interaction independently of the conditions required for the screening in living cells. If a positive extract was found, further purification of the active principle could be performed and a purified compound, or family of compounds, later be evaluated in living cells. This strategy could also allow the derivatization of compounds in order to modify properties such as

solubility. Additionally, it has to be taken into account that PPIs might be hard to disrupt [4], specially considering the presence of well-defined binding pockets in the interface of the PPIs [37]. Small compounds present in the extracts would be expected to bind at PPI sites with very low affinity, due to their solvent exposure and limited contact area [38]. Thus, more likely to be avoided by inhibitors before the interaction takes place rather than disrupted, several inducible screening systems have been developed in order to add the inhibitory compound before allowing PPI to happen [4]. In a similar way, to circumvent this main disadvantage of searching inhibitors of PPIs by using BRET, in our system of mixing lysates expressing the PPI partners would allow the reconstitution of an interaction once the inhibitory compound has been added.

The first criterion used for the selection of fusion protein combinations to be tested in lysates was based on the BRET signal obtained in living cells. However, some of the PPIs that presented strong signal in living cells, such as P0-Rluc/P1β-EYFP and Rluc-P0/P1β-EYFP (Fig. 2b), P0-Rluc/EYFP-P2α (Fig. 2c), Rluc-P2β/P0-EYFP (Fig. 2d), Rluc-P2β/P1α-EYFP, P2β-Rluc/EYFP-P1α, and P2β-Rluc/P1α-EYFP (Fig. 2e), gave no BRET signal in lysates. In addition, we detected hyperbolic BRET signal from lysates for the combinations Rluc-P1α/P0-EYFP and P1α-Rluc/P0-EYFP (Fig. 4a), Rluc-P1β/P0-EYFP (Fig. 4b) and Rluc-P2α/P0-EYFP, which presented no signal in living cells. Similarly, some combinations of mRNA processing proteins presented no BRET signal in lysates (Supplementary Figure 2), other combinations, such as SF3b155-Rluc/EYFP-p14, p14-Rluc/SF3b155-EYFP and Rluc-p14/SF3b155-EYFP (Fig. 5c), and Y14-Rluc/EYFP-Mago, Y14-Rluc/Mago-EYFP- Rluc-Y14/EYFP-Mago, and Rluc-Mago/EYFP-Y14 (Fig. 5), presented BRET signal exclusively in cells, and finally, few combinations, for instance Rluc-U2AF65/EYFP-SF1, U2AF65-Rluc/EYFP-SF1, and U2AF65-Rluc/SF1-EYFP (Fig. 5a) or Rluc-Y14/Mago-EYFP (Fig. 5b), gave BRET signal only in lysates. Altogether, our observations suggested that it is not possible to establish a correlation between the BRET results from living cells and lysates. This fact underscores the importance of analyzing the greatest number of fusion protein combinations for each interaction pair in order to establish the best combination to be used in the screening. Finally, to confirm that the system could be turned off, a bacterially expressed His-Sf3b155$^{1\text{-}270}$ was used as competitor of the Sf3b155-Rluc/p14-EYFP interaction and a significant attenuation in the BRET signal was observed.

Overall, our results strongly suggested that a BRET assay for library screening could be developed to identify PPI inhibitors that may be useful for the treatment of *T. cruzi*.

Experimental Procedure

Entry Vector Construction

The open reading frames (ORFs) were amplified by PCR and purified from agarose gels. The pCRTM8/GW/TOPO®TA entry vector (Gateway System, Thermo Fisher) was used to clone the following ORF: P0$^{212\text{-}323}$, P1α, P1β, P2α, P2β, SF1, FIP1, CpsF30, p14, Mago, Y14, U2AF65$^{614\text{-}841}$, Sf3b155$^{1\text{-}270}$. The cloning reaction was initiated by adding 3 µL of each PCR product, 0.5 µL of the entry vector, and 1.5 µL of mili-Q water to 1 µL of saline solution provided by the manufacturer. The mixture was incubated at room temperature for 5 min. Vectors were amplified in *E. coli* in the presence of 100 µg/mL of spectinomycin. Primers used are shown in Supplementary Table 1.

BRET Destinations Plasmids

BRET plasmids pEYFP-N1 (Clontech), pEYFP-C1 (Clontech), pRluc-N3(h) (BioSignal Packard), and pRluc-C2(h) (BioSignal Packard) were converted to Gateway (ThermoFisher) destination vector using a Gateway Vector Conversion System cassette cloned by restriction into the SmaI site at the multiple cloning site of the vector.

BRET Destination Vector Subcloning

The gene of interest was transferred from the pCRTM8 entry vector to specific BRET destination plasmid, by LR Clonase® II (Thermo Fisher)-mediated recombination, following manufacturer protocol. Briefly, 200 ng of each plasmid was mixed with LR clonase and incubated for 1 h at room temperature. Reaction was stopped by addition of proteinase K (2 µg/µl) (Thermo Fisher), and the mixture was incubated 10 min at 37 °C. *E. coli* competent bacteria were transformed with 3 µL of the recombination reaction and seeded in LB-agar medium in the presence of the appropriate antibiotic. Plasmids were sequence-verified.

BRET Saturation Assay in Living Cells

HEK 293T cells were seeded into 12-well plates at a density of 5×10^5 cells per well 1 day before transfection. Cells were co-transfected with a total amount of 0.8 µg of DNA. The energy donor amount was fixed at 0.4 µg per well, and increasing amounts of the energy acceptor were added (0.1, 0.2, 0.3, and 0.4 µg; a vacant plasmid was used when necessary to complete 0.8 µg of DNA in total). 24 h later, cells were seeded in white 96-well plates in triplicate. After another 24 h, medium was removed and 60 µl of PBS pH 7,4 1X containing the coelenterazine h (5 µM final concentration) (Thermo Fisher) was added. Cells were incubated at

37 °C for 15 min covered from the light. Light emitted by the donor and acceptor was simultaneously measured in a Mithras LB 940 Multimode Microplate Reader (Berthold technologies) with a 485 ± 10 nm filter for luciferase and a 530 ± 12.5 nm filter for EYFP. The background signal due to the overlap of the energy donor emission at the energy acceptor wavelength was determined by repeating the procedure with cells expressing only the energy donor protein. The data show the average values of triplicates from three independent experiments. BRET values (expressed as milliBRET) were calculated as follows:

$$mBRET = \left[\left(\frac{Light\ \ emitted\ \ by\ \ acceptor\ _{530\ \mathrm{nm}}}{Luminescence_{485}}\right) - \left(\frac{Light\ \ emitted\ \ by\ \ acceptor_{530\ \mathrm{nm}}}{Luminescence_{485}}\right)_{Background}\right] \times 1000.$$

BRET Saturation Assay in Lysates

HEK 293T cells were seeded into 10-cm-diameter cell culture dishes at a density of 5×10^6 cells 1 day before transfection. The cells were transfected with 12 µg of the corresponding BRET plasmid and 48 h later were mechanically lysed. Briefly, cells were carefully rinsed with 1X PBS pH 7.4, scraped with 1.5 ml of fresh 1X PBS, and collected into appropriate conical centrifuge tubes. After centrifugation for 5 min at 450×*g* at 4 °C, the supernatant was discarded. The packed cell volume (PCV) was estimated, and the cells were gently resuspended in five PVC of hypotonic lysis buffer. After 15 min of incubation on ice, the cells were centrifuged for 5 min at 420×*g* at 4 °C. The supernatant was discarded, and the cells were gently resuspended in 2xPVC of hypotonic lysis buffer. The cell suspension was slowly drawn into a syringe with a 27-gauge hypodermic needle and then ejected in a single rapid stroke. This procedure was repeated five times. The suspension was centrifuged for 20 min at 11000×*g* and 4 °C. The supernatant was transferred to tubes in 30 µl aliquots and flash freeze with liquid nitrogen. The aliquots were stored at − 80 °C until used. For the saturation assay, total protein was quantified and fixed amount of the energy donor (corresponding to 150,000 relative light subunits of luciferase activity) was incubated for 30 min with increasing amounts of the energy acceptor (5, 15, 20, and 30 µg/well) in a final volume of 50 µL of hypotonic lysis buffer (10 mM Hepes, 1.5 mM MgCl2, 10 mM KCl, 1 M DTT, and 1X protease inhibitor cocktail) in white 96-well plates. Afterward, 50 µL of a 5-µM solution of coelenterazine h in hypotonic lysis buffer was added to each well and incubated for 30 min guarded from the light. The experiment was carried out by triplicate. Light emitted at donor and acceptor wavelengths was simultaneously measured as stated above. The background signal was determined by measuring the energy donor signal in the absence of the energy acceptor. BRET values were calculated as stated before. The data show the average values of triplicates from three independent experiments.

His-Sf3b155 Expression and Purification

Escherichia coli BL21(DE3) cells were chemically transformed with pDEST17-Sf3b155$^{1\text{-}270}$ and cultured in LB plates containing ampicillin henicol. A single colony was inoculated into LB medium and grown overnight at 37 °C. The bacterial culture was diluted and grown up to an A_{600} of 0.6. Protein expression was induced by the addition of 1 mM isopropyl β-D-1-thiogalactopyranoside for 2 h at 37 °C. Cells were harvested by centrifugation at 5000×*g* for 10 min and resuspended in lysis buffer containing 50 mM Tris–HCl (pH 7), 50 mM NaCl, cOmplete™ Protease Inhibitor Cocktail (Roche). Cells were lysed by the addition of lysozyme (1 mg/ml), β-mercaptoethanol (5 mM), Sarkosyl (1%), and Triton X-100 (2%) for 30 min at room temperature and sonicated (four cycles of 20 s). Soluble fraction was recovered after centrifugation at 9000 rpm for 20 min at 4 °C. Lysates were incubated with nickel–nitrilotriacetic acid (Qiagen) according to the manufacturer's instructions. Unbound protein was washed with 50 mM Tris–HCl, 150 mM NaCl, 50 mM imidazole, and 5 mM β-mercaptoethanol, and proteins were eluted with 3 ml of buffer containing 50 mM Tris–HCl (pH 7), 150 mM NaCl, 300 mM imidazole, and 5 mM β-mercaptoethanol. Purified proteins were stored in 15% glycerol at − 80 °C.

Validation of the Sf3b1551-270-Rluc/p14-EYFP Interaction Specificity

The amount of protein corresponding to 150.000 RLU of the energy donor (Sf3b155$^{1\text{-}270}$-Rluc) was co-incubated with 20 µg of the energy acceptor (p14-EYFP) for 30 min in white 96-well plates, either in the presence or absence of 5 µg of the His-Sf3b155$^{1\text{-}270}$ as competitor. Subsequently, 50 µL of a 5-µM solution of coelenterazine h in hypotonic lysis buffer was added. BRET signal was measured as stated before.

Curve Fitting

All curves were generated with Graphpad Prism v6.01 software. An exponential fit was applied selecting the option of one-phase association and the least-squares fitting method. R^2 values are showed in Supplementary Table 2.

Compliance with Ethical Standards

Conflict of interest The authors declare that they have no conflict of interest.

Ethical Approval This article does not contain any studies with human participants or animals performed by any of the authors.

References

1. Ngounou Wetie, A. G., Sokolowska, I., Woods, A. G., Roy, U., Loo, J. A., & Darie, C. C. (2013). Investigation of stable and transient protein-protein interactions: Past, present, and future. *Proteomics, 13*(3–4), 538–557.
2. Dimri, S., Basu, S., & De, A. (2016). Use of BRET to study protein–protein interactions In Vitro and In Vivo. *Methods in Molecular Biology, 1443,* 57–78.
3. Bacart, J., Corbel, C., Jockers, R., Bach, S., & Couturier, C. (2008). The BRET technology and its application to screening assays. *Biotechnology Journal, 3*(3), 311–324.
4. Couturier, C., & Deprez, B. (2012). Setting up a bioluminescence resonance energy transfer high throughput screening assay to search for protein/protein interaction inhibitors in mammalian cells. *Frontiers in Endocrinology (Lausanne), 3,* 100.
5. Corbel, C., Sartini, S., Levati, E., Colas, P., Maillet, L., Couturier, C., et al. (2017). Screening for protein–protein interaction inhibitors using a bioluminescence resonance energy Transfer (BRET)-based assay in yeast. *SLAS Discovery, 22*(6), 751–759.
6. Bern, C. (2015). Chagas' disease. *New England Journal of Medicine, 373*(19), 1882.
7. Corbel, C., Wang, Q., Bousserouel, H., Hamdi, A., Zhang, B., Lozach, O., et al. (2011). First BRET-based screening assay performed in budding yeast leads to the discovery of CDK5/p25 interaction inhibitors. *Biotechnology Journal, 6*(7), 860–870.
8. Dragulescu-Andrasi, A., Chan, C. T., De, A., Massoud, T. F., & Gambhir, S. S. (2011). Bioluminescence resonance energy transfer (BRET) imaging of protein-protein interactions within deep tissues of living subjects. *Proceedings of the National Academy of Sciences, 108*(29), 12060–12065.
9. Cui, B., Wang, Y., Song, Y., Wang, T., Li, C., Wei, Y., et al. (2014). Bioluminescence resonance energy transfer system for measuring dynamic protein-protein interactions in bacteria. *MBio, 5*(3), e01050-14.
10. Griss, R., Schena, A., Reymond, L., Patiny, L., Werner, D., Tinberg, C. E., et al. (2014). Bioluminescent sensor proteins for point-of-care therapeutic drug monitoring. *Nature Chemical Biology, 10*(7), 598–603.
11. Xu, Y., Piston, D. W., & Johnson, C. H. (1999). A bioluminescence resonance energy transfer (BRET) system: application to interacting circadian clock proteins. *Proceedings of the National Academy of Sciences, 96*(1), 151–156.
12. Wu, P., & Brand, L. (1994). Resonance energy transfer: methods and applications. *Analytical Biochemistry, 218*(1), 1–13.
13. Kasprzak, A. A. (2007). The use of FRET in the analysis of motor protein structure. *Methods in Molecular Biology, 392,* 183–197.
14. Xu, Y., Kanauchi, A., von Arnim, A. G., Piston, D. W., & Johnson, C. H. (2003). Bioluminescence resonance energy transfer: monitoring protein-protein interactions in living cells. *Methods in Enzymology, 360,* 289–301.
15. Sun, S., Yang, X., Wang, Y., & Shen, X. (2016). In vivo analysis of protein-protein interactions with bioluminescence resonance energy transfer (BRET): Progress and prospects. *International Journal of Molecular Sciences, 17*(10), 1704.
16. Loening, A. M., Wu, A. M., & Gambhir, S. S. (2007). Red-shifted Renilla reniformis luciferase variants for imaging in living subjects. *Nature Methods, 4*(8), 641–643.
17. Liljas, A. (1991). Comparative biochemistry and biophysics of ribosomal proteins. *International Review of Cytology, 124,* 103–136.
18. Levin, M. J., Vazquez, M., Kaplan, D., & Schijman, A. G. (1993). The *Trypanosoma cruzi* ribosomal P protein family: Classification and antigenicity. *Parasitology Today, 9*(10), 381–384.
19. Ayub, M. J., Atwood, J., Nuccio, A., Tarleton, R., & Levin, M. J. (2009). Proteomic analysis of the *Trypanosoma cruzi* ribosomal proteins. *Biochemical and Biophysical Research Communications, 382*(1), 30–34.
20. Smulski, C. R., Longhi, S. A., Ayub, M. J., Edreira, M. M., Simonetti, L., Gomez, K. A., et al. (2011). Interaction map of the *Trypanosoma cruzi* ribosomal P protein complex (stalk) and the elongation factor 2. *Journal of Molecular Recognition, 24*(2), 359–370.
21. De Gaudenzi, J. G., Noe, G., Campo, V. A., Frasch, A. C., & Cassola, A. (2011). Gene expression regulation in trypanosomatids. *Essays in Biochemistry, 51,* 31–46.
22. Liang, X. H., Haritan, A., Uliel, S., & Michaeli, S. (2003). Trans and cis splicing in trypanosomatids: mechanism, factors, and regulation. *Eukaryotic Cell, 2*(5), 830–840.
23. Wahl, M. C., Will, C. L., & Luhrmann, R. (2009). The spliceosome: Design principles of a dynamic RNP machine. *Cell, 136*(4), 701–718.
24. Rino, J., Desterro, J. M., Pacheco, T. R., Gadella, T. W., Jr., & Carmo-Fonseca, M. (2008). Splicing factors SF1 and U2AF associate in extraspliceosomal complexes. *Molecular and Cellular Biology, 28*(9), 3045–3057.
25. Vazquez, M. P., Mualem, D., Bercovich, N., Stern, M. Z., Nyambega, B., Barda, O., et al. (2009). Functional characterization and protein-protein interactions of trypanosome splicing factors U2AF35, U2AF65 and SF1. *Molecular and Biochemical Parasitology, 164*(2), 137–146.
26. Avila, M. L., Bercovich, N., Westergaard, G., Levin, M. J., & Vazquez, M. P. (2007). Mapping of the protein-binding interface between splicing factors SF3b155 and p14 of *Trypanosoma cruzi*. *Biochemical and Biophysical Research Communications, 364*(1), 26–32.
27. Rymond, B. (2007). Targeting the spliceosome. *Nature Chemical Biology, 3*(9), 533–535.
28. Bercovich, N., Levin, M. J., & Vazquez, M. P. (2009). The FIP-1 like polyadenylation factor in trypanosomes and the structural basis for its interaction with CPSF30. *Biochemical and Biophysical Research Communications, 380*(4), 850–855.
29. Le Hir, H., Sauliere, J., & Wang, Z. (2016). The exon junction complex as a node of post-transcriptional networks. *Nature Reviews Molecular Cell Biology, 17*(1), 41–54.
30. Bercovich, N., Levin, M. J., Clayton, C., & Vazquez, M. P. (2009). Identification of core components of the exon junction complex in trypanosomes. *Molecular and Biochemical Parasitology, 166*(2), 190–193.
31. Juri Ayub, M., Smulski, C. R., Nyambega, B., Bercovich, N., Masiga, D., Vazquez, M. P., et al. (2005). Protein–protein interaction map of the *Trypanosoma cruzi* ribosomal P protein complex. *Gene, 357*(2), 129–136.
32. Maldonado, E., Soriano-Garcia, M., Moreno, A., Cabrera, N., Garza-Ramos, G., de Gomez-Puyou, M., et al. (1998). Differences in the intersubunit contacts in triosephosphate isomerase from two closely related pathogenic trypanosomes. *Journal of Molecular Biology, 283*(1), 193–203.
33. Olivares-Illana, V., Rodriguez-Romero, A., Becker, I., Berzunza, M., Garcia, J., Perez-Montfort, R., et al. (2007). Perturbation of

the dimer interface of triosephosphate isomerase and its effect on *Trypanosoma cruzi*. *PLoS Neglected Tropical Diseases, 1*(1), e1.
34. Gayosso-De-Lucio, J., Torres-Valencia, M., Rojo-Dominguez, A., Najera-Pena, H., Aguirre-Lopez, B., Salas-Pacheco, J., et al. (2009). Selective inactivation of triosephosphate isomerase from *Trypanosoma cruzi* by brevifolin carboxylate derivatives isolated from *Geranium bellum* Rose. *Bioorganic & Medicinal Chemistry Letters, 19*(20), 5936–5939.
35. Tellez-Valencia, A., Olivares-Illana, V., Hernandez-Santoyo, A., Perez-Montfort, R., Costas, M., Rodriguez-Romero, A., et al. (2004). Inactivation of triosephosphate isomerase from *Trypanosoma cruzi* by an agent that perturbs its dimer interface. *Journal of Molecular Biology, 341*(5), 1355–1365.
36. Aguilera, E., Varela, J., Birriel, E., Serna, E., Torres, S., Yaluff, G., et al. (2016). Potent and selective inhibitors of *Trypanosoma cruzi* triosephosphate isomerase with concomitant inhibition of cruzipain: Inhibition of parasite growth through multitarget activity. *ChemMedChem, 11*(12), 1328–1338.
37. Cierpicki, T., & Grembecka, J. (2015). Targeting protein-protein interactions in hematologic malignancies: still a challenge or a great opportunity for future therapies? *Immunological Reviews, 263*(1), 279–301.
38. Valkov, E., Sharpe, T., Marsh, M., Greive, S., & Hyvonen, M. (2012). Targeting protein-protein interactions and fragment-based drug discovery. *Topics in Current Chemistry, 317,* 145–179.